

Measurement of polarization observables in neutral double pion photoproduction off the proton with the CBELSA/TAPS experiment

Tobias Seifen^{1,*} for the CBELSA/TAPS collaboration

¹Helmholtz-Institut für Strahlen- und Kernphysik, Universität Bonn, Nussallee 14-16, 53115 Bonn, Germany

Abstract. Data on the reaction $\gamma p \rightarrow p\pi^0\pi^0$ were taken with the CBELSA/TAPS experiment at ELSA where linearly polarized photons impinged on a transversely polarized butanol target. Target asymmetries and double polarization observables were extracted and entered the BnGa-PWA. Systematic differences in the branching ratios of N^* and Δ^* resonances hint at the internal structure of these states.

1 Introduction

The excited states in hadron spectroscopy are broad and overlapping. Hence, a partial wave analysis (PWA) needs to be performed where polarization observables are essential to resolve ambiguities in the PWA solutions. Resonance contributions cannot be extracted from the (unpolarized) cross section alone. At higher center-of-mass energy the importance of multi-meson final states increases and cascading decays via intermediate resonances occur.

The neutral double pion channel is especially advantageous compared to the charged pion channel, since it suffers much less from non-resonant contributions: There is no diffractive ρ production, no Kroll-Ruderman term (direct $\Delta\pi$ production) and t -channel processes are suppressed, thus enhancing the sensitivity to resonance contributions.

2 Experimental Setup

The CBELSA/TAPS experiment allows the measurement of double polarization observables. Electrons with an energy of 3.2 GeV from the Electron Stretcher Accelerator ELSA [1] produced linearly polarized photons (maximal polarization degree of 66 % at $E_\gamma = 850$ MeV) by means of coherent bremsstrahlung from a diamond crystal [2]. The energy-tagged photons hit a transversely polarized butanol (C_4H_9OH) target [3] (mean polarization degree of 74 %). The Crystal Barrel calorimeter [4] and the Forward Plug, consisting out of 1320 CsI(Tl) crystals, surround the target. Together with the TAPS calorimeter [5] (216 BaF₂ crystals), for polar angles below 12°, nearly the full solid angle was covered.

For the identification of charged particles, a scintillating fiber detector [6] (513 fibers in three layers) surrounding the target and plastic scintillator counters in front of the Forward Plug and TAPS crystals were used.

Furthermore, a gas-cherenkov detector located between the Crystal Barrel and TAPS calorimeters was used

*e-mail: seifen@hiskp.uni-bonn.de

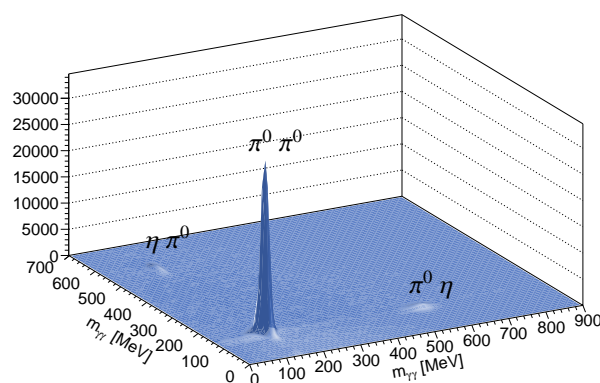


Figure 1. Invariant mass of one photon pair versus the other after the angular cuts and a cut on the missing proton mass.

to suppress electro-magnetic background on the trigger level.

3 Data Selection

To select events stemming from the reaction $\gamma p \rightarrow p\pi^0\pi^0 \rightarrow p4\gamma$ five hits were required. Four of these hits had to be neutral and be registered in the calorimeters. For the proton candidate a hit in one of the charge-sensitive detectors, giving only a direction, was sufficient. Cuts on the proton direction relative to the vector sum of the photon momenta were applied, requiring the proton and the photons to be back to back in the center of mass system. The invariant mass of one $\gamma\gamma$ -pair plotted versus the other is depicted in Fig. 1. The $p\pi^0\pi^0$ final state, as well as the $p\pi^0\eta$ final state are clearly visible. The final selection employs a kinematic fit including an anti-cut on the $p\pi^0\eta$ final state, with which the combinatorial background still present in Fig. 1 can be eliminated. A cut on the confi-

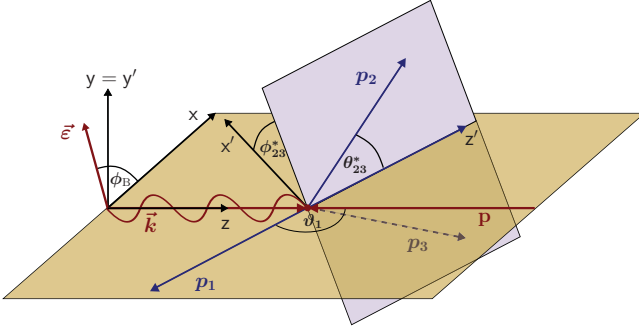


Figure 2. Kinematics of the 3-body final state, showing the reaction plane spanned by the incoming photon and one of the final state particles (p_1) and the decay plane spanned by the remaining final state particles (p_2 and p_3). For the $p\pi^0\pi^0$ final state there are two choices for particles 1(23): $p(\pi^0\pi^0)$ and $\pi^0(p\pi^0)$.

dence level (> 0.1) acted as a joint mass cut on the pions and the missing proton.

After applying all cuts, the amount of background varies kinematically dependent from well below 1% to about 5%. Globally, a background contamination of about 1.5% was reached.

4 Analysis

When considering multi-meson final states, like in the reaction $\gamma p \rightarrow p\pi^0\pi^0$, additional kinematic variables are needed to describe the kinematics compared to the case of single meson photoproduction. In total five kinematic variables are used (cf. Fig. 2): Apart from the beam energy E_γ and the scattering angle $\cos\vartheta_1$ those are the invariant mass m_{23} and two angles, ϕ_{23}^* and θ_{23}^* .

The polarized cross section of double pseudoscalar meson photoproduction (only taking linear beam polarization and transverse target polarization into account) is given by [7]:

$$\begin{aligned} \frac{d\sigma}{d\Omega} = \frac{d\sigma_0}{d\Omega} \cdot \{ & 1 + \Lambda_x \cdot P_x + \Lambda_y \cdot P_y \\ & + \delta_\ell \sin(2\phi_B) \cdot I_{\text{eff}}^s + \delta_\ell \cos(2\phi_B) \cdot I_{\text{eff}}^c \\ & + \Lambda_x \delta_\ell \sin(2\phi_B) \cdot P_x^s + \Lambda_y \delta_\ell \sin(2\phi_B) \cdot P_y^s \\ & + \Lambda_x \delta_\ell \cos(2\phi_B) \cdot P_x^c + \Lambda_y \delta_\ell \cos(2\phi_B) \cdot P_y^c \}, \end{aligned} \quad (1)$$

where Λ_x , Λ_y are the target polarizations in / perpendicular to the reaction plane, and δ_ℓ the beam polarization (with angle ϕ_B to the reaction plane). The beam asymmetries I_{eff}^s and I_{eff}^c contain the beam asymmetries from the bound protons in the carbon and oxygen nuclei and are therefore not considered here further.

In a quasi 2-body approach, where p_2 and p_3 are added up, half of the polarization observables (namely P_x , P_x^c , and P_y^s) vanish exactly, while the others are often identified with their single meson counter parts ($P_y = T$, $P_x^s = -H$, and $P_y^c = -\tilde{P}$).

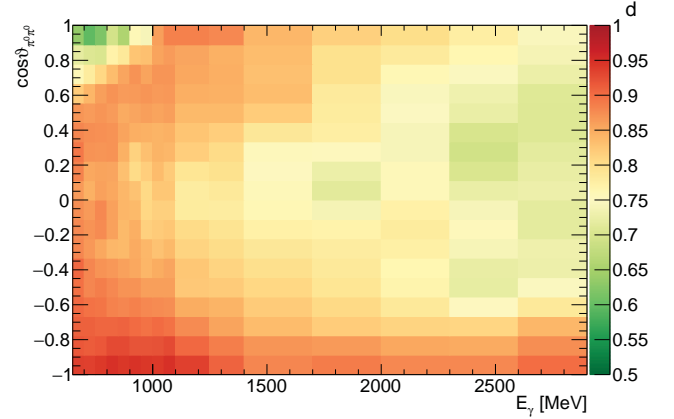


Figure 3. Dilution factor d depending on E_γ and $\cos\vartheta_{\pi^0\pi^0}$.

4.1 Dilution factor

Since the butanol target also contains bound nucleons in the carbon and oxygen nuclei which can not be polarized, the target polarization is effectively reduced by the fraction of polarizable (free) protons. This so-called dilution factor depends on the kinematic variables as well as the applied cuts, since the bound nucleons are subject to Fermi motion. Therefore, the effectively remaining carbon and oxygen dilution was determined experimentally with the use of a carbon foam target of approximately the same area density as the carbon and oxygen nuclei in the butanol target.

The resulting dilution factor is depicted in Fig. 3 as a function of beam energy E_γ and $\cos\vartheta_{\pi^0\pi^0}$. Especially for lower energies ($E_\gamma \lesssim 1100$ MeV) it reaches values of around 0.9.

4.2 Results

The polarization observables were determined in each kinematic bin by means of an event-based maximum-likelihood fit to the ϕ -distribution of the events. Possible detector asymmetries were expanded in a Fourier series and coefficients which interfere with the polarization observables were fitted.

As an example, results for the target asymmetry T in the quasi 2-body approach are shown in Fig. 4 as a function of $\cos\vartheta_{\pi^0\pi^0}$ in the beam energy range of 650 MeV to 2600 MeV. The data points are plotted together with predictions from the 2π -MAID [8] and the BnGa-PWA [9], as well as a new BnGa solution which contains this data. Clear deviations are seen to the MAID predictions over the whole energy range while the 2014 BnGa solution describes the data fairly well at lower energies. At higher energies (above 1700 MeV) larger deviations become apparent. The new BnGa solution describes the target asymmetry quite well over the whole energy range.

Fig. 5 shows the target asymmetry P_x as a function of $\phi_{\pi^0\pi^0}^*$. Due to parity conservation P_x has to be odd under the transformation $\phi^* \mapsto 2\pi - \phi^*$. Thus P_x vanishes when integrating over ϕ^* . The open symbols in Fig. 5 make use

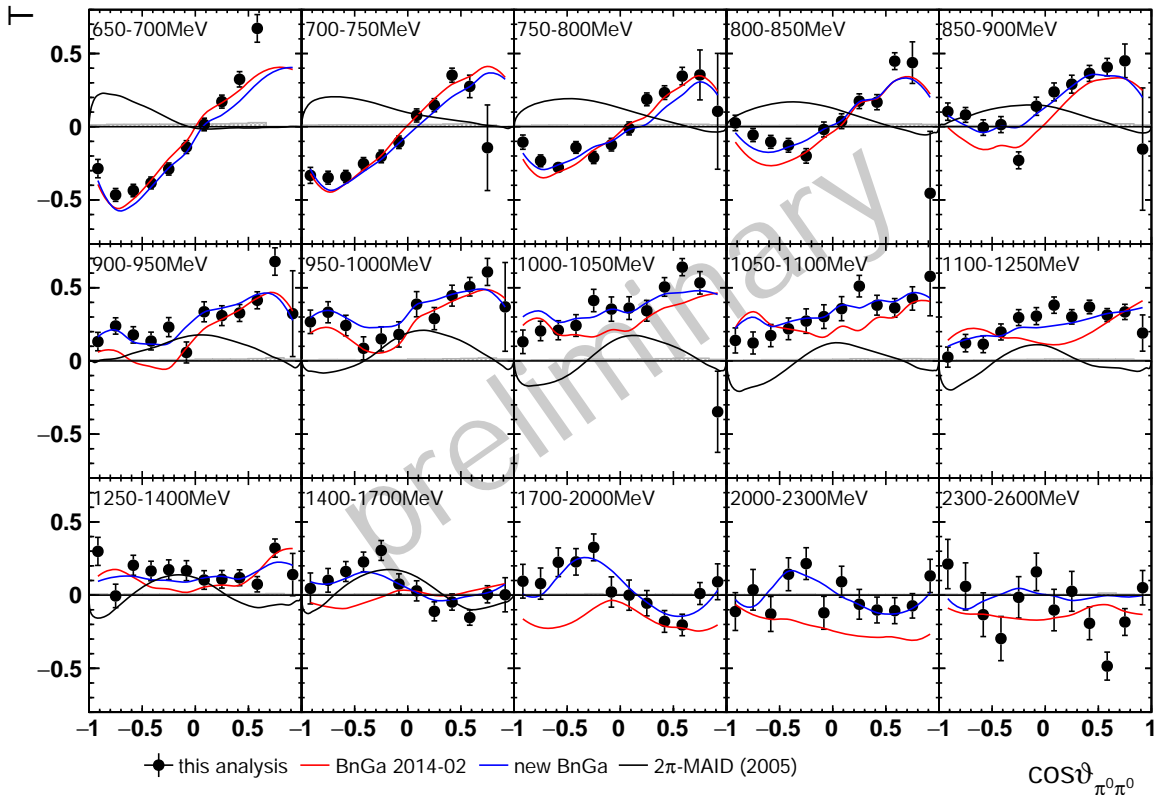


Figure 4. Targetasymmetry T as a function of beam energy E_γ and $\cos \vartheta_{\pi^0\pi^0}$.

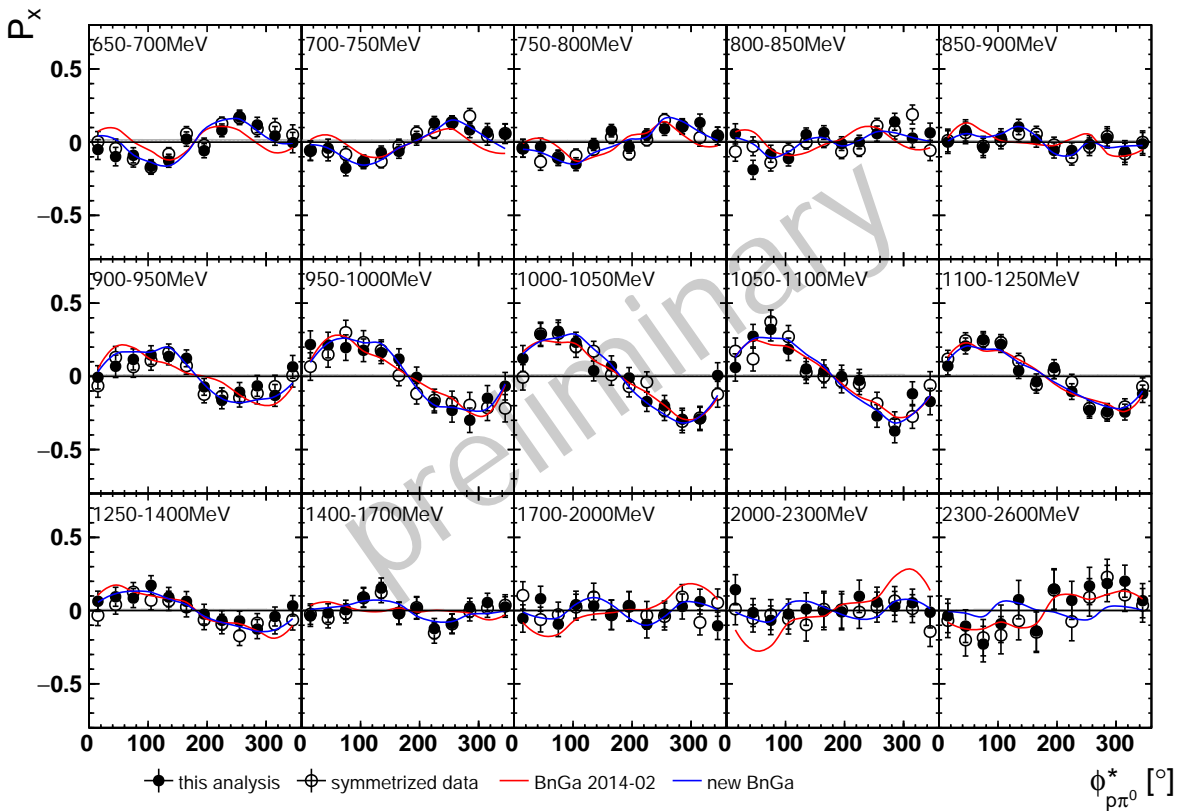


Figure 5. Targetasymmetry P_x as a function of beam energy E_γ and $\phi_{\rho\pi^0}^*$.

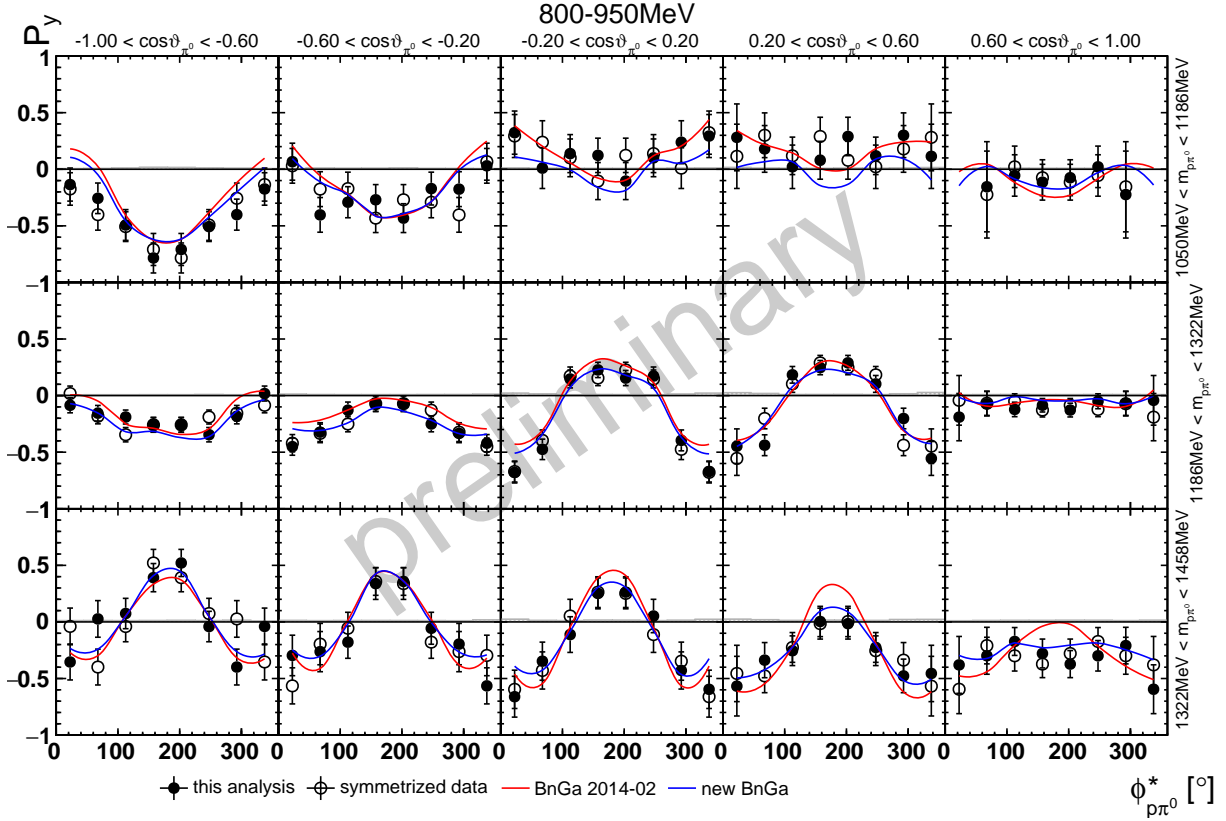


Figure 6. Targetasymmetry P_y as a function of $\phi_{p\pi^0}^*$ in the energy bin (800 – 950) MeV. Within a row the $\cos\vartheta_{\pi^0}$ is varied, within a column the invariant mass $m_{p\pi^0}$. Only a single energy bin is shown here.

of the symmetry property, which is clearly fulfilled in the data.

For beam energies below 1250 MeV the statistics were high enough to determine the target asymmetries in a 4-dimensional analysis. Fig. 6 shows an example of the target asymmetry P_y in one energy bin (800 MeV < E_γ < 950 MeV), where $\phi_{p\pi^0}^*$ is plotted on the x -axis, $\cos\vartheta_{\pi^0}$ is varied within the rows and $m_{p\pi^0}$ within the columns. It becomes immediately apparent that the observables can change significantly from bin to bin. This information is not fully contained in the partially integrated observables.

4.3 PWA

The extracted polarization observables were considered in a new solution of the BnGa coupled-channel partial wave analysis which includes all major data of pion and photo-induced reactions off protons and neutrons [10]. Investigating the decay modes of the excited baryon states, it becomes apparent that some resonances have a significant branching ratio into excited hadrons while others decay dominantly into ground state nucleons or deltas. The structure of the baryon wave function might explain this behavior.

Expanding the spatial wave function of an excited baryon in a harmonic oscillator basis (with oscillators λ and ϱ) allows to group the wave functions into three classes. First, there are wave functions where only one

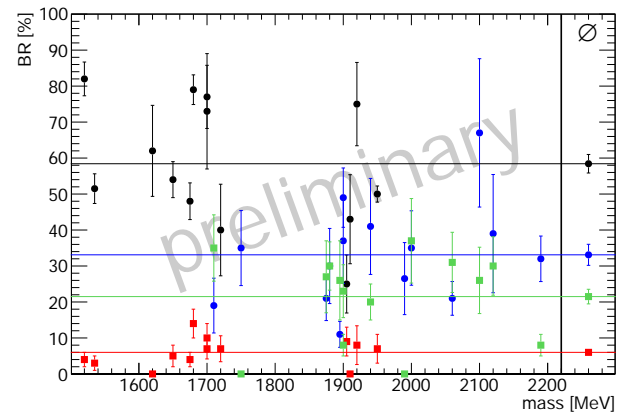


Figure 7. Branching ratios of resonances included in the BnGa-PWA are illustrated. One-oscillator resonances decaying into the ground states ($N\pi$ or $\Delta\pi$) are shown as black dots, decays into excited resonances ($N(1520)\pi$, $N(1535)\pi$, $N(1680)\pi$, or $N\sigma$) as red squares. Mixed-oscillator states decaying into the ground states are shown as blue dots, those decaying into the excited states as green squares. Additionally, the average branching ratios are shown on the right and as colored lines.

oscillator (either λ or ϱ) is excited, e.g. $\ell_\lambda = 2, \ell_\varrho = 0$. Then, there are those where both oscillators are excited simultaneously, e.g. $\ell_\lambda = 1 = \ell_\varrho$. And lastly, there is the coherent sum of the previous two classes, i.e. part of the

wave function has only one oscillator excited and part of the wave function has both oscillators excited simultaneously.

Resonances of the second class, which only have a spatial wave function where both oscillators are in an excited state (belonging to the antisymmetric SU(6) 20-plet), have not been found experimentally yet.

Those resonances with only one excited oscillator were found to decay dominantly (nearly 60 % on average) into the ground states $N\pi$ or $\Delta\pi$ (black dots in Fig. 7) while the branching ratios for decays into excited states ($N(1520)\pi$, $N(1535)\pi$, $N(1680)\pi$, or $N\sigma$) are small (red squares), 6 % on average. On the other hand, resonances which additionally have a part in their wave function with both oscillators excited, have a similar branching ratio for decays into the ground states (blue dots in Fig. 7) and excited states (green squares), about 33 % to about 22 % on average.

5 Summary

New results on the measurement of (double) polarization observables in the reaction $\gamma p \rightarrow p\pi^0\pi^0$ with the CBELSA/TAPS experiment were reported, utilizing linearly polarized photons and a transversely polarized butanol target. The data were included in the data base of the BnGa coupled channel partial wave analysis. The new

PWA solution hints at the structure of the wave function: Compared to resonances whose wave function have only one excited oscillator, resonances whose wave function have parts with both oscillators in an excited state, have a significant branching ratio into an excited baryon or meson followed by a subsequent decay into the three-particle final state.

References

- [1] W. Hillert, *Eur. Phys. J. A* **28**, 139-148 (2006).
- [2] D. Elsner *et al.*, *Eur. Phys. J. A* **39**, 373 (2009).
- [3] Ch. Bradtke, H. Dutz, H. Peschel *et al.*, *Nucl. Instr. Meth. A* **436**, 430-442 (1999).
- [4] E. Aker *et al.*, *Nucl. Instr. Meth. A* **321**, 69-108 (1992).
- [5] R. Novotny, *IEEE Trans. Nucl. Sci. NS* **38**, 379-385 (1991).
- [6] G. Suft *et al.*, *Nucl. Instr. Meth. A* **531**, 416-424 (2005)
- [7] W. Roberts, T. Oed, *Phys. Rev. C* **71**, 055201 (2005).
- [8] H. Arenhövel, A. Fix, *Eur. Phys. J. A* **25**, 115-135 (2005).
- [9] V. Sokhoyan *et al.*, *Eur. Phys. J. A* **51**, no.8, 95 (2015)
Erratum: [*Eur. Phys. J. A* **51** no.12, 187 (2015)]
- [10] Webpage on baryon spectroscopy of the BnGa group: pwa.hiskp.uni-bonn.de/baryon_x.htm